Water Research 187 (2020) 116442

Contents lists available at ScienceDirect

Water Research

journal homepage: www.elsevier.com/locate/watres

Seasonal contrast of particulate organic carbon (POC) characteristics in the Geum and Seomjin estuary systems (South Korea) revealed by carbon isotope ($\delta^{13}C$ and $\Delta^{14}C$) analyses

Sujin Kang[a], Jung-Hyun Kim[b,*], Ji Hwan Hwang[c], Yeon Sik Bong[d], Jong-Sik Ryu[e], Kyung-Hoon Shin[a,*]

[a] Hanyang University ERICA, 55 Hanyangdaehak-ro, Sangnok-gu, Ansan-si, Gyeonggi-do 15588, South Korea
[b] KOPRI Korea Polar Research Institute, 26 Songdomirae-ro, Yeonsu-gu, Incheon 21990, South Korea
[c] Graduate School of Analytical Science and Technology, Chungnam National University, Daejeon 34134, South Korea
[d] Division of Earth and Environmental Sciences, Korea Basic Science Institute, Chungbuk 28119, South Korea
[e] Department of Earth and Environmental Sciences, Pukyong National University, Busan 48513, South Korea

ARTICLE INFO

Article history:
Received 3 July 2020
Revised 18 September 2020
Accepted 20 September 2020
Available online 21 September 2020

Keywords:
Particulate organic carbon
Dissolved inorganic carbon
Carbon isotopes
Sediment resuspension
Geum estuary
Seomjin estuary

ABSTRACT

In this study, we newly investigated surface water samples collected in two contrasting Korean estuary systems (i.e., closed Geum and open Seomjin estuaries) along a salinity gradient in winter (December) in 2016. The main objectives were to determine the source of particulate organic carbon (POC) in winter and to assess the environmental factors inducing seasonal differences in POC characteristics. Concentrations and dual carbon isotopes ($\delta^{13}C$ and $\Delta^{14}C$) of POC were analyzed together with concentrations and stable carbon isotopes ($\delta^{13}C$) of dissolved inorganic carbon (DIC) and compared with those obtained in summer (August) in 2016. Our study provided a new insight that for both estuarine systems, the seasonal contrast in POC characteristics was associated with stronger wind-induced estuarine sediment resuspensions in winter than in summer providing a greater contribution of aged POC to the total POC pool in winter.

1. Introduction

Rivers are the vital link between land and sea (e.g., Hedges et al., 1997; Bauer and Bianchi, 2011). Riverine carbons are transferred to the sea in various forms, such as dissolved and particulate organic carbon (DOC and POC), largely because of soil leaching and erosion (Meybeck, 1982). World rivers transport approximately 0.4×10^{15} g C yr^{-1} from land to sea, primarily through estuaries, out of which approximately 38% is in particulate form (Meybeck, 1982; Ludwig and Probst, 1996; Hedges et al., 1997). Estuarine POC may be derived from allochthonous (i.e., terrestrial plant detritus and soils and marine primary production) and autochthonous (i.e., *in situ* aquatic production) sources (Bauer et al., 2013). The stable carbon isotope ($\delta^{13}C$) has been used for tracing the source of POC in estuaries combined with the radiocarbon isotope ($\Delta^{14}C$) which provides additional information on the source and the reactivity of POC (e.g., Raymond and Bauer, 2001). Organic carbon (OC) delivery via the river–estuary–sea continuum may vary seasonally due to biotic and abiotic processes including primary productivity, river discharge, and physical mixing (e.g., Bianchi and Duan, 2006; Cai et al., 2016; Guo et al., 2015; Hoffman and Bronk, 2006). For instance, thermal and saline stratifications prevent a vertical mixing in summer due to a large temperature difference between warmer surface water and cold bottom water and a stronger episodic riverine freshwater input under the Asian monsoon system (Lee et al., 2010).

The Geum River is the third largest river in South Korea flowing into the mid-eastern Yellow Sea. It has a length of 398 km and a drainage area of 9914 km^2 (Water Resources Management Information System, WAMIS, http://www.wamis.go.kr). Its mean annual water discharge was 324 m^3 s^{-1}, ranging from 102.4 m^3 s^{-1} in February to 841.1 m^3 s^{-1} in July 2016 (Water Environment Information System, WEIS, http://water.nier.go.kr). The Seomjin River discharges into the South Sea of Korea (northern extension of the East China Sea). The length of the Seomjin River was 222 km with a drainage basin area of 4914 km^2 (WAMIS). Its mean annual water discharge was 55.5 m^3 s^{-1}, showing a minimum value of 21.9 m^3 s^{-1} in August 2016 and a maximum value of 140.5 m^3 s^{-1} in October 2016 (WEIS). An estuary dam was built in the Geum estu-

* Corresponding author.
E-mail addresses: jhkim123@kopri.re.kr (J.-H. Kim), shinkh@hanyang.ac.kr (K.-H. Shin).

https://doi.org/10.1016/j.watres.2020.116442
0043-1354/

ary in 1990. In contrast, the Seomjin estuary was an open estuary without a dam.

A previous study of the Geum and Seomjin rivers showed that the catchment area-normalized fluxes of POC were 4.0×10^{-4} tC km^{-2} yr^{-1} in the Geum River and 5.2×10^{-4} tC km^{-2} yr^{-1} in the Seomjin River between May 2016 and May 2018 (Kang et al., 2019). The POC flux was more weakly associated with the water discharge in the Geum River than in the Seomjin River, indicating that the estuary dam of the Geum River influenced the POC fluxes into the estuary by modifying the water residence times through an artificial drainage control in the reservoir. Higher $\delta^{13}C_{POC}$ and $\Delta^{14}C_{POC}$ values in the surface water samples collected along a salinity gradient in the Geum estuary than those in the Seomjin estuary in August 2016 indicated that phytoplankton-derived POC was the main contributor to the total POC pool in the reservoir of the Geum estuary due to an enhanced phytoplankton bloom associate with an increase in water residence time by the estuary dam, whereas terrestrial-derived POC was predominantly transported by the Seomjin River (Kang et al., 2020). Accordingly, the estuary dam of the Geum River altered the source and reactivity of POC in the reservoir in summer, which could have been exported to the adjacent estuary when the water gate was open. However, the seasonal contrast of POC characteristics along a salinity gradient has not been yet determined in either estuary system.

In this study, we newly investigated surface water samples collected along a salinity gradient from the Geum (closed) and Seomjin (open) estuary systems in winter (December) in 2016. We analyzed the concentrations and dual carbon isotopes ($\delta^{13}C$ and $\Delta^{14}C$) of POC together with the concentrations and stable carbon isotopes ($\delta^{13}C$) of dissolved inorganic carbon (DIC) and compared them with those obtained in summer (August) in 2016. The main objectives of this study were to determine the source of POC in winter and thus to evaluate the environmental factors inducing the seasonal differences in POC characteristics in two contrasting Korean estuary systems.

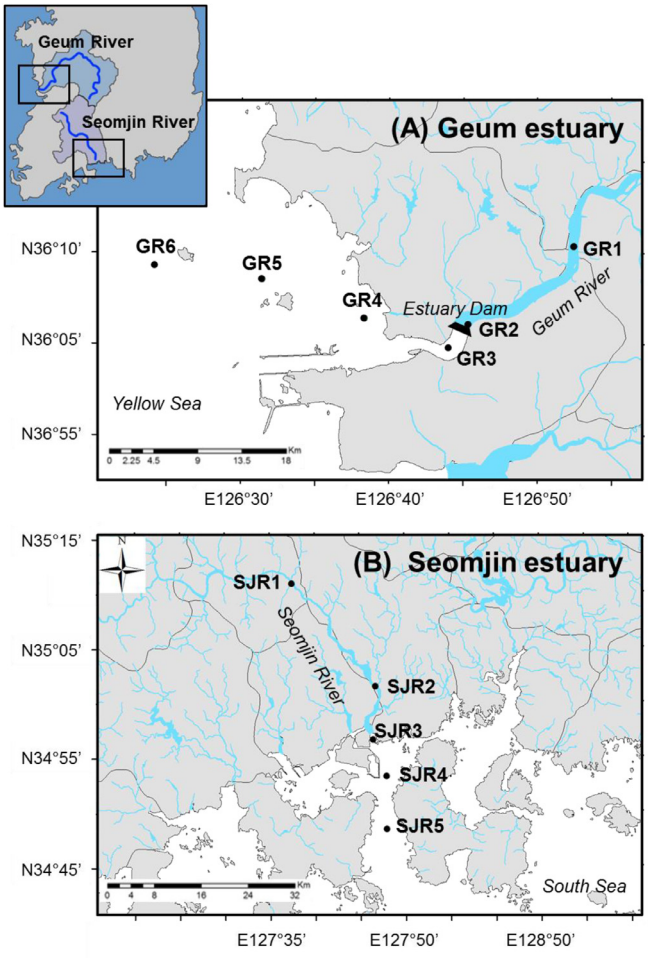

Fig. 1. Location of the sampling sites in (A) the Geum estuary and (B) the Seomjin estuary.

2. Materials and methods

2.1. Sample collection

Surface water samples were collected along a salinity gradient from the land (i.e., last gauging station of each river) to sea sites in the Geum and Seomjin estuary systems in August and December 2016 (Figs. 1 and 2). Surface water was taken directly into a high-density polyethylene carboy through Tygon tubing using an aspirator system at or near high-tide conditions. Approximately 0.1–2 L of water was filtered through a pre-combusted (450°C, 5h) and pre-weighed 0.45 μm glass fiber filter (Macherey-Nagel, Dueren, Germany). The filters were freeze-dried and then weighed to calculate the total suspended matter (TSM) concentration. They were also used for the concentration and isotope ($\delta^{13}C$ and $\Delta^{14}C$) analysis of POC. Filtrates were collected in high-density polyethylene bottles for the analysis of total alkalinity and 125 mL glass bottles with 85% H_3PO_4 for the $\delta^{13}C$ analysis of DIC.

2.2. Hydrological and water parameters

The river water discharge and monthly mean precipitation data for the Geum and Seomjin basins in 2016 were obtained from WEIS and the Korea Meteorological Administration (KMA, http://www.kma.go.kr), respectively. The daily averaged wind speed data were obtained from the Gunsan and Gwangyang stations in August and December 2016 (KMA, http://www.kma.go.kr). In situ water parameters (temperature, salinity, pH, and turbidity) were measured using a Hydrolab DS5 multi-parameter water quality sonde (OTT Hydromet, Kempten, Germany) during the sampling campaigns in August and December 2016.

2.3. Chemical parameters

Total alkalinity was measured using a T50 titrator (Mettler Toledo, Schwerzenbach, Switzerland). The DIC concentration was calculated using PHREEQC (computer program for speciation, reaction-path, advective-transport, and inverse geochemical calculations, U.S. Geological Survey, Earth Science Information Center, Denver, USA), which considered the measured water temperature, pH, and total alkalinity (cf. Shin et al., 2015). The stable isotope ratios of DIC ($\delta^{13}C_{DIC}$) were analyzed with extracted CO_2 gas using a dual-inlet isotope ratio mass spectrometer (Isoprime, GV Instrument, Manchester, UK). The POC concentrations and the stable carbon isotopes of POC ($\delta^{13}C_{POC}$) were analyzed following the same procedure of Kang et al. (2020). The radiocarbon analysis of POC ($\Delta^{14}C_{POC}$) was conducted at the National Ocean Science Accelerator Mass Spectrometry Facility of the Woods Hole Oceanographic Institution (NOSAMS, Woods Hole, USA) and the Alfred Wegener Institute (AWI, Bremerhaven, Germany), following their standard routines.

2.4. Conservative mixing model calculation

The DIC and POC concentrations and the isotope compositions of $\delta^{13}C_{DIC}$, $\delta^{13}C_{POC}$, and $\Delta^{14}C_{POC}$ resulting from a mix of freshwa-

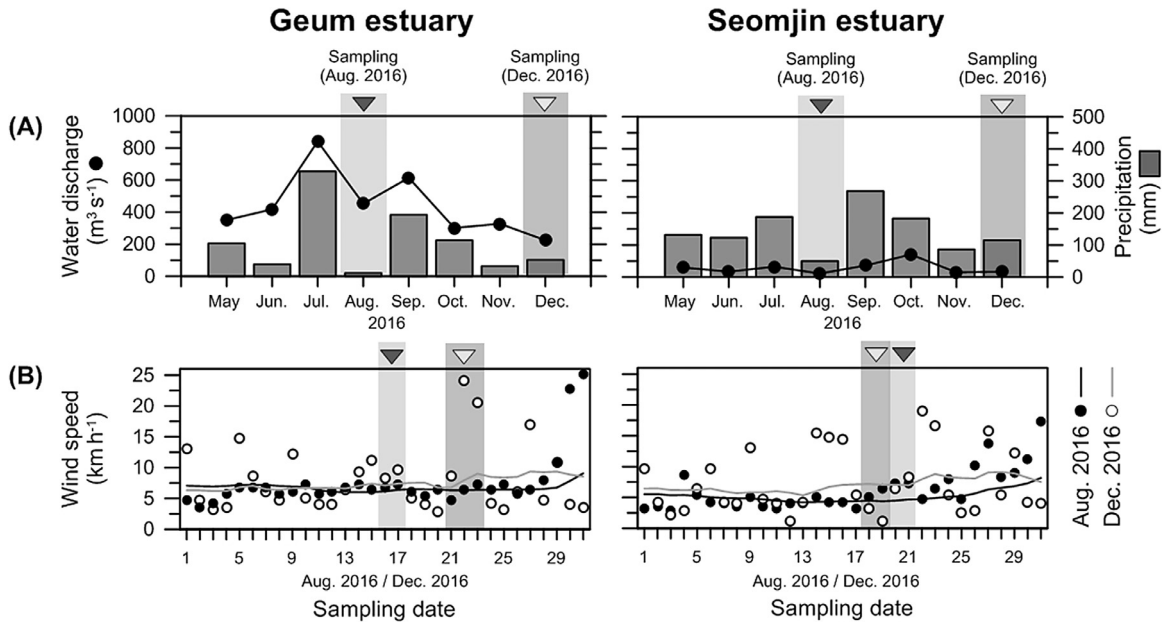

Fig. 2. Variation in (A) water discharges ($m^3\ s^{-1}$) and monthly precipitations (mm) in the Geum and Seomjin estuaries in 2016 and (B) daily wind speeds (circles) and average wind speeds of 14 days (lines) (km h^{-1}) in the Geum and Seomjin estuaries in August and December 2016. Note that the water discharge and precipitation data were taken from Kang et al. (2019).

ter and seawater were calculated using the following equations (cf. Samanta et al., 2015; Wang et al., 2016; Bhavya et al., 2018),

$$S_{mix} = S_f F_f + S_m(1 - F_f) \quad (1)$$

$$[C]_{mix} = [C]_f F_f + [C]_m\left(1 - F_f\right) \quad (2)$$

$$I_{mix} = [C]_f I_f F_f + [C]_m I_m (1 - F_f)/[C]_f F_f + [C]_m (1 - F_f) \quad (3)$$

where S_{mix} is the measured salinity at each site and S_f and S_m represent the freshwater and seawater end member values of the salinity, respectively. *[C]* is the concentration of DIC and POC and *I* indicates the isotopes of each carbon species (i.e., $\delta^{13}C_{DIC}$, $\delta^{13}C_{POC}$, and $\Delta^{14}C_{POC}$). Subscripts *mix* represents the expected value through conservative mixing, whereas *f* and *m* indicate freshwater and seawater, respectively. The data from GR1 in the Geum River and SJR1 in the Seomjin River were used as the freshwater end-member values, whereas the data from GR6 and SJR5 were used as the seawater end-member values for each estuary system (Tables 1 and 2, see also Fig. 1). The concentration and isotope deviations between the measured and modeled values ($\Delta[C]$ and $\Delta[I]$, respectively) were calculated as follows (cf. Samanta et al., 2015),

$$\Delta[C] = \left([C]_{sample} - [C]_{mix}\right)/[C]_{mix} \quad (4)$$

$$\Delta[I] = I_{sample} - I_{mix} \quad (5)$$

where $[C]_{sample}$ and I_{sample} are the measured values and $[C]_{mix}$ and I_{mix} are the modeled values.

2.4. Statistical analysis

To determine the relationship among the different data sets, the Pearson test (R) was performed using IBM SPSS 25 (SPSS Inc., IBM Corp., Armonk, New York, USA). Probabilities (p) were determined, and a p value of < 0.05 was considered to be significant.

3. Results

3.1. Geum estuary

At the time of sampling in December 2016, the wind speeds were higher than those in August 2016 (Fig. 2), and the water masses were characterized by a temperature range of 4.9–9.7°C, a salinity range of 0.3–35.0 psu, a pH range of 6.5–9.7, and a turbidity range of 261–450 NTU (Figs. 3 and 4). The surface water temperature in December 2016 (on average, 8.6 ± 1.5°C) was much lower than in August 2016 (on average, 30.9 ± 1.1°C) showing similar temperatures before and after the dam (Fig. 4A). However, other water parameters (i.e., salinity, pH, and total alkalinity) were drastically changed before and after the dam in two sampling periods (Figs. 4B-D). The turbidity in December 2016 (on average, 436 ± 16 NTU) was much higher than in August 2016 (on average, 48 ± 18 NTU) showing a similar before and after the dam (Fig. 4E). In general, the TSM concentrations were lower before the dam than after the dam, showing similar ranges in summer and winter (Fig. 4F). The DIC concentrations (11.1–27.1 mgC L^{-1} in August 2016 and 17.2–28.2 mgC L^{-1} in December 2016) were also lower before the dam than after the dam for both sampling periods, but with higher concentrations in the reservoir in winter than in summer (Fig. 5A). In contrast, the POC concentrations in December 2016 (0.3–2.7 mgC L^{-1}) were slightly higher before the dam than after the dam, showing a smaller contrast compared to that in summer (Fig. 5B). The $\delta^{13}C_{DIC}$ values were lower before the dam than after the dam for both sampling periods, ranging from −12.0‰ to 0.3‰ (Fig. 6A). The $\delta^{13}C_{POC}$ values in December 2016 were between −32.5‰ and −25.3‰, showing different trends along the salinity gradient for two sampling periods (Fig. 6B). The $\Delta^{14}C_{POC}$ values in December 2016 (−351.0‰ to −87.0‰) showed a larger difference between before and after the dam compared to that in August 2016 (Fig. 6C).

3.2. Seomjin estuary

The average wind speed of previous 14 days at the time of sampling was higher in December 2016 than in August 2016 (Fig. 2B).

Table 1
Sample information and environmental parameters considered in this study. Note that the water temperature, salinity, pH, and TSM data from all sampling sites in August 2016 were taken from Kang et al. (2020) and from GR1 and SJR1 in December 2016 were taken from Kang et al. (2019).

Study area	Sampling date (YYYY-MM-DD)	Sampling site	Latitude	Longitude	Water temperature (°C)	Salinity (ppt)	pH	Total alkalinity (meq L^{-1})	Turbidity (NTU)	TSM concentration (mg L^{-1})
Geum estuary	2016-08-17	GR1	36.0899	126.8741	31.6	0.2	9.9	1.34	71	25.19±4.1
	2016-08-17	GR2	36.0187	126.7551	31.6	0.1	9.2	1.18	51	12.20±0.4
	2016-08-17	GR3	36.9993	126.7269	31.6	26.7	8.0	1.97	67	95.87±4.1
	2016-08-17	GR4	36.0242	126.6385	31.5	33.4	7.6	2.13	33	57.00±5.4
	2016-08-17	GR5	36.0596	126.5235	30.2	33.4	7.8	2.18	29	24.67±5.2
	2016-08-17	GR6	36.6327	126.1112	29.0	34.0	7.8	2.19	38	10.45±2.6
	2016-12-22	GR1	36.0899	126.8741	9.4	0.3	8.9	1.47	451	7.72±0.7
	2016-12-22	GR2	36.0187	126.7551	9.7	0.3	7.7	1.41	445	6.59±0.5
	2016-12-22	GR3	36.9993	126.7269	6.9	26.5	7.6	1.67	429	20.89
	2016-12-22	GR4	36.0242	126.6385	6.5	32.4	7.6	2.16	408	70.15±5.8
	2016-12-22	GR5	36.0596	126.5235	9.7	33.5	7.7	2.22	445	29.77±1.3
	2016-12-22	GR6	36.6327	126.1112	9.2	34.9	7.7	2.22	435	29.55±0.2
Seomjin estuary	2016-08-20	SJR1	35.1825	127.6246	29.9	0.0	9.0	0.88	72	2.20±0.2
	2016-08-20	SJR2	35.0257	127.7785	29.9	21.9	7.2	1.63	78	33.49±0.5
	2016-08-20	SJR3	34.9444	127.7733	27.2	34.3	7.4	2.09	6	27.17±0.9
	2016-08-20	SJR4	34.8891	127.7979	26.5	35.2	7.6	2.13	53	31.61±9.0
	2016-08-20	SJR5	34.8084	127.7979	27.5	34.8	7.8	2.14	51	21.05±7.5
	2016-12-19	SJR1	35.1825	127.6246	7.7	0.1	8.4	0.81	75	2.28±2.3
	2016-12-19	SJR2	35.0257	127.7785	7.2	14.7	7.7	1.34	467	17.90±0.4
	2016-12-19	SJR3	34.9444	127.7733	11.0	32.6	7.8	2.02	289	26.10
	2016-12-19	SJR4	34.8891	127.7979	11.8	34.8	7.8	2.18	309	25.83±1.4
	2016-12-19	SJR5	34.8084	127.7979	11.7	35.2	7.9	2.19	273	31.88±1.3

Table 2
Results obtained in this study. The nd abbreviation denotes "not determined". Note that the POC concentration, $\delta^{13}C_{POC}$, and $\Delta^{14}C_{POC}$ data from all sampling sites in August 2016 were taken from Kang et al. (2020), and the POC concentration and $\delta^{13}C_{POC}$ data from GR1 and SJR1 in December 2016 were taken from Kang et al. (2019).

Study area	Sampling date (YYYY-MM-DD)	Sampling site	DIC concentration (mgC L^{-1})	POC concentration (mgC L^{-1})	$\delta^{13}C_{DIC}$ (‰ VPDB)	$\delta^{13}C_{POC}$ (‰ VPDB)	$\Delta^{14}C_{POC}$ (‰)
Geum estuary	2016-08-17	GR1	11.08	12.70±2.05	−9.18	−19.36±0.14	−51.12
	2016-08-17	GR2	12.84	4.20±0.83	−12.04	−22.87±0.24	−81.65
	2016-08-17	GR3	23.87	4.83±0.46	−1.02	−20.97±0.12	−98.20
	2016-08-17	GR4	26.93	2.26±0.19	−0.78	−23.94±0.29	−82.44
	2016-08-17	GR5	26.84	1.72±0.15	0.10	−21.35±0.48	−74.46
	2016-08-17	GR6	27.08	0.19±0.04	0.28	−23.48±0.21	−48.11
	2016-12-22	GR1	17.18	2.65±0.11	−8.31	−28.73±0.29	−87.03
	2016-12-22	GR2	17.96	2.18±0.15	−8.74	−32.49±0.07	−101.84
	2016-12-22	GR3	21.70	1.13±0.04	nd	−30.68±0.10	−221.83
	2016-12-22	GR4	27.68	1.03	nd	−26.32	−298.04
	2016-12-22	GR5	28.14	0.36	−1.86	−26.35	−351.00
	2016-12-22	GR6	28.24	0.26	−1.83	−25.33	−202.27
Seomjin estuary	2016-08-20	SJR1	9.89	0.76±0.22	−12.65	−29.10±0.16	−188.25
	2016-08-20	SJR2	22.27	1.04±0.02	−4.02	−23.04±0.36	−105.03
	2016-08-20	SJR3	27.06	0.79±0.07	−1.54	−22.28±0.33	−51.41
	2016-08-20	SJR4	27.00	0.90±0.11	−0.47	−21.05±0.42	−81.62
	2016-08-20	SJR5	26.38	0.90±0.05	0.00	−21.80±0.10	−103.44
	2016-12-19	SJR1	9.72	0.33±0.02	−9.29	−26.61±0.02	−187.27
	2016-12-19	SJR2	16.99	0.49±0.09	−5.44	−28.96±0.27	−302.19
	2016-12-19	SJR3	25.20	0.48±0.07	−1.81	−26.62±0.51	−241.06
	2016-12-19	SJR4	27.22	0.32±0.02	−1.34	−26.63±0.19	−261.54
	2016-12-19	SJR5	27.12	0.32±0.02	−1.24	−26.55±0.23	−263.43

Vertical profiles of the water temperature, salinity, and turbidity indicated variations of 7.2–11.8°C, 0.1–35.2 psu, and 78–467 NTU in December 2016 (Figs. 3C and D). The surface water temperature showed a decreasing trend in August 2016 but an increasing trend in December 2016, with the much lower average value of 9.9 ± 2.3°C in December 2016 (Fig. 4A). However, other water parameters (i.e., salinity, pH, and total alkalinity) showed the same trends for both sampling periods (Figs. 4C and D). The turbidity and the TSM concentration showed a gradual increase toward the sea sites in both sampling periods (Figs. 4D and E) but the turbidity showed a larger difference between August 2016 (on average, 52 ± 28 NTU) and December 2016 (on average, 283 ± 140 NTU). The DIC concentration also showed an increasing trend toward the sea sites, having a similar range of 9.9 to 27.1 mgC L^{-1} in August 2016 and 9.7 to 27.2 mgC L^{-1} in December 2016 (Fig. 5A). In contrast, the POC concentrations did not reveal a clear trend, with the lower average concentration of 0.4 ± 0.1 mgC L^{-1} in December 2016 than in August 2016 (Fig. 5B). The $\delta^{13}C_{DIC}$ values increased toward the sea sites for both sampling periods, ranging from −12.7‰ to 0‰ (Fig. 6A). In December 2016, neither $\delta^{13}C_{POC}$ nor $\Delta^{14}C_{POC}$ showed a clear trend, with generally lower values (−29.0 to −26.6‰ and −302.2 to −187.3‰, respectively) than those in August 2016 (Figs. 6 B and C).

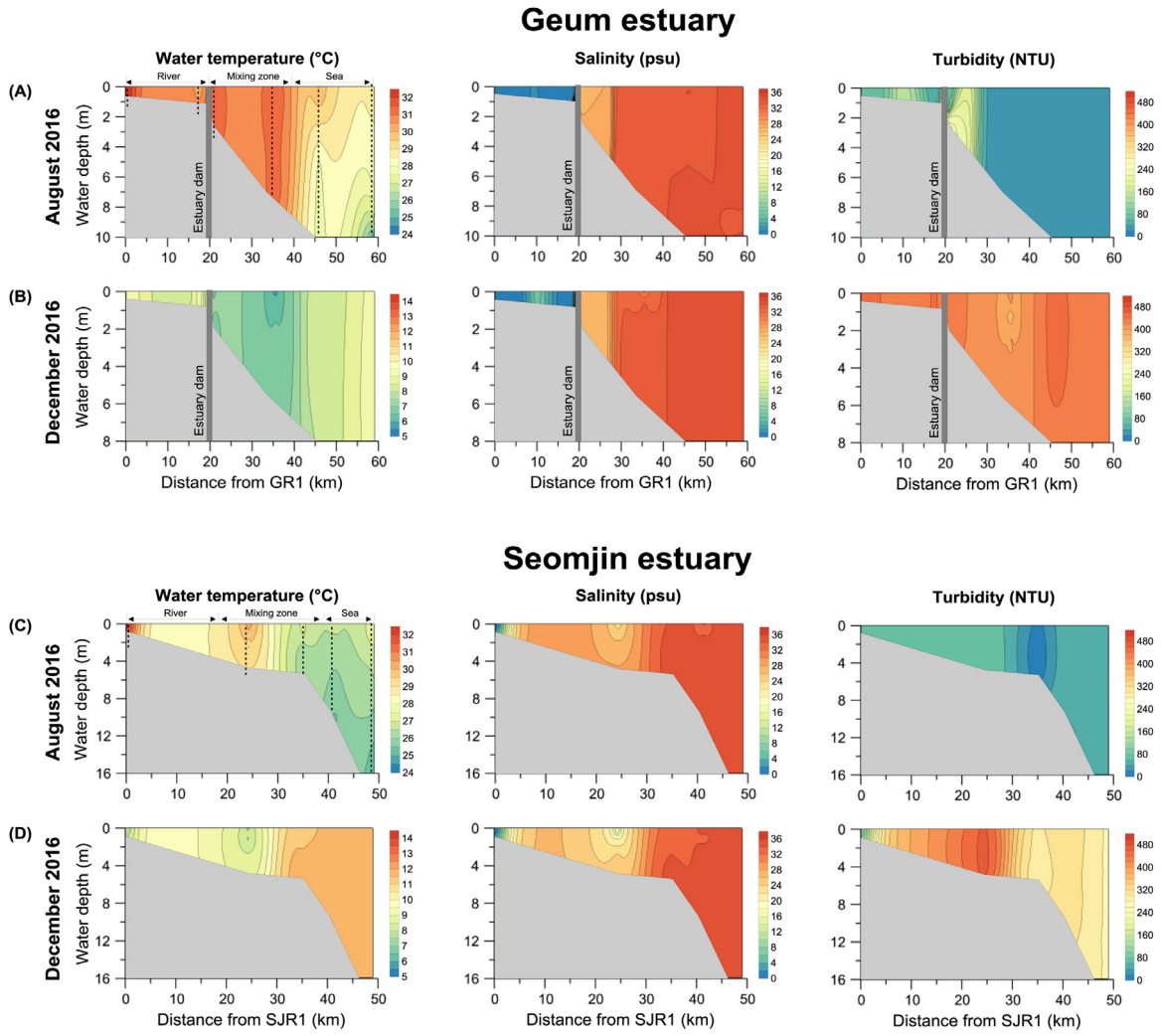

Fig. 3. Vertical distribution pattern of water parameters (water temperature (°C), salinity (psu), and turbidity (NTU)) in (A) August and (B) December 2016 in the Geum estuary and in (C) August and (D) December 2016 in the Seomjin estuary. The in situ measurement sites are indicated by black dotted lines.

4. Discussion

4.1. Riverine POC sources

At the Geum River sites (GR1 and GR2), the POC concentrations were higher in August 2016 than in December 2016 (Fig. 5B). In a natural river system, the POC concentration associated with soil erosion is commonly related to the TSM concentration, which is strongly controlled by hydrodynamic processes (e.g., Wood, 1977; Beusen et al., 2005; Bouchez et al., 2011; Guo et al., 2015; Wu et al., 2018). At GR1 and GR2, the TSM concentrations were slightly higher in August 2016 than in December 2016 (Fig. 4F), which is consistent with the higher water discharge in August 2016 compared with December 2016 (Fig. 2A). Thus, it appears that the input of soil-derived POC into the Geum River was higher in August 2016 than in December 2016. Notably, the POC concentration was lower at GR2 than at GR1 in August 2016, whereas both sites showed similar POC concentrations in December 2016 (Fig. 5B). The POC concentration at GR2 was also much lower than the modeled value in August 2016. This suggests that in addition to the soil-derived POC supply, an additional input from other POC sources might have contributed to the total riverine POC pool. Indeed, a previous study at GR1 showed that a heavy riverine algae bloom occurred in the Geum River in August 2016 (Kang et al., 2019). Hence, it appears that the contribution of phytoplankton-derived POC to the total POC pool was higher at GR1 than at GR2 in August 2016, associated with the estuary dam, which altered the natural land–sea continuum (Kang et al., 2020). At the Seomjin River site (SJR1), the POC concentration was also higher in August 2016 than in December 2016 (Fig. 5B), although the TSM concentrations and water discharges were similar in both seasons (Figs. 2B and 4F). This might be due to a higher contribution of plant-derived POC to the TSM pool in August 2016 than in December 2016, whereas the variation in soil-derived POC was minor in both seasons.

The $\delta^{13}C_{POC}$ values at GR1 and GR2 were higher in August 2016 (−22.9 to −19.4‰) than in December 2016 (−32.5 to −28.7‰, Fig. 6B). The fact that the $\delta^{13}C_{POC}$ values were higher in August 2016 than in December 2016 appears to be associated with the higher contribution of autochthonous POC due to increased primary phytoplankton production (Kang et al., 2019, 2020). In contrast, the lower $\delta^{13}C_{POC}$ values in December 2016 are comparable with the signatures of the terrestrial C_3 plants, which use the Calvin pathway of carbon fixation with $\delta^{13}C$ values of average −28‰ in the range of −32 to −24‰ (e.g., Peterson and Fry, 1987; Meyers, 1997; Marwick et al., 2015). Indeed, C_3 plants such as *Phragmites* spp., *Salix* spp., and *Rubus parvifolius* are dominant in the Geum River watershed in spring and summer (S. Lee et al.,

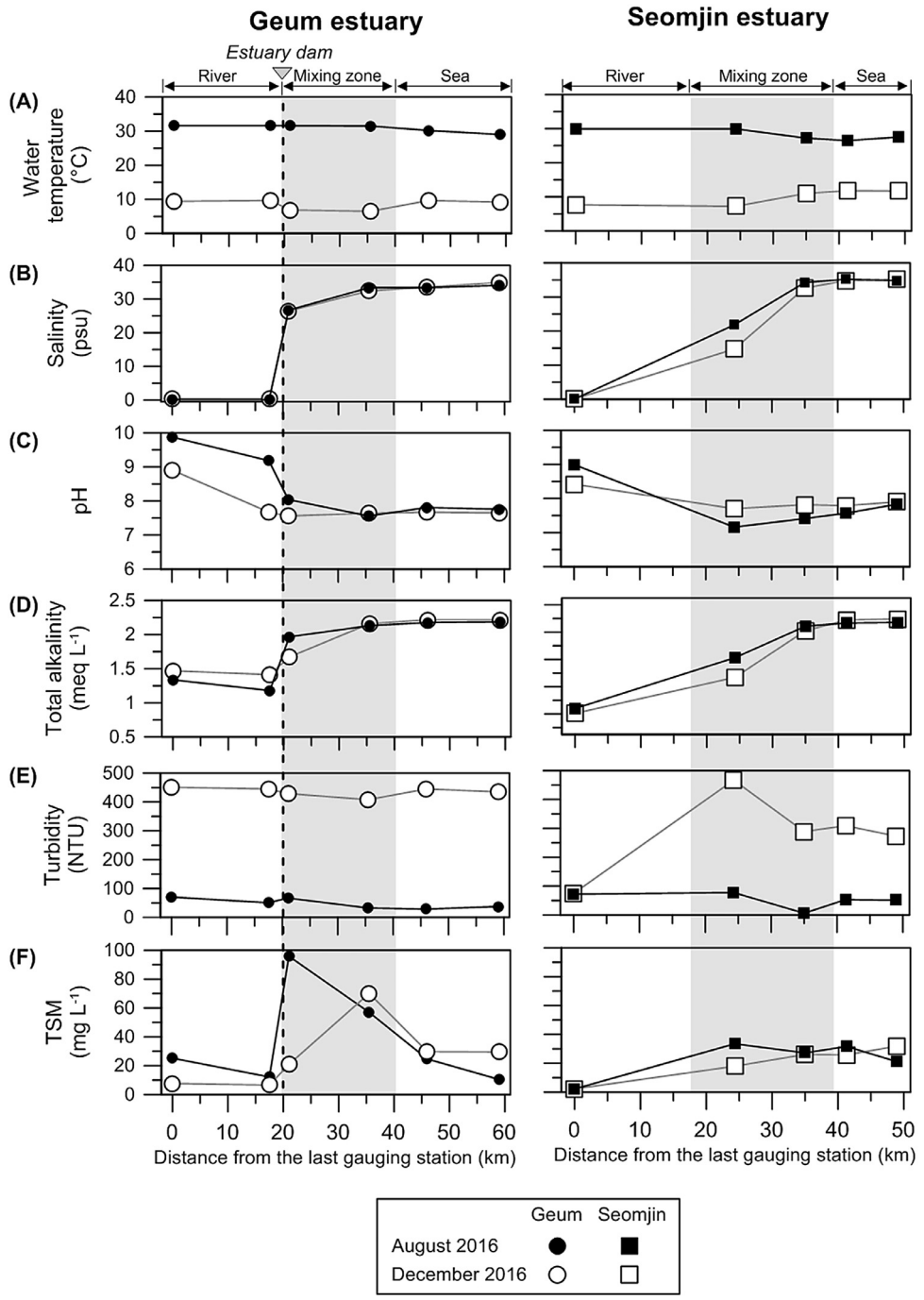

Fig. 4. Variation in (A) water temperature (°C), (B) salinity (psu), (C) pH, (D) total alkalinity (meq L^{-1}), (E) turbidity (NTU), and (F) TSM concentration (mg L^{-1}).

2018). Thus, lower $\delta^{13}C_{POC}$ values of winter samples suggest that influence of C_3 plant debris inputs to the total POC pool was stronger in winter in the absence of a phytoplankton bloom. Notably, the $\delta^{13}C_{POC}$ values at GR2 for both seasons were lower than those at GR1 as well as the modeled values (Fig. 6B). This seems to be associated with higher contributions of phytoplankton-derived POC with enriched $\delta^{13}C_{POC}$ values to the total POC pool at GR1 than GR2 in both seasons. At SJR1, the $\delta^{13}C_{POC}$ value was lower in August 2016 (−29.1‰) than in December 2016 (−26.6‰, Fig. 6B). Considering the fact that the POC concentration in August 2016 was higher than in December 2016 (see Fig. 5B) with similar TSM concentrations and water discharges (Fig. 2B), as mentioned above, the lower $\delta^{13}C_{POC}$ value in August 2016 as compared with that in December 2016 seems to be due to the higher contribution of fresher plant-derived POC to the total POC pool, whereas the soil-derived POC contributions were similar in both seasons. In fact, the $\delta^{13}C_{POC}$ value in August 2016 was in the range of the signatures of the common C_3 reed (*Phragmites australis*, −27 to −29‰), which is dominant in the Seomjin River in spring and summer (Min and Je, 2002; Choi et al., 2005; Kang et al., 2020). Hence, it seems that the contribution of C_3 plants to the total POC pool in the Seomjin River was higher in August 2016 than in December 2016.

Evidence supporting the $\delta^{13}C_{POC}$ signatures discussed above can be found in the $\delta^{13}C$ characteristics of DIC, which play a critical role in the primary productivity as a source of bioavailable carbon for aquatic plant photosynthesis (e.g., Sand-Jensen et al., 1992;

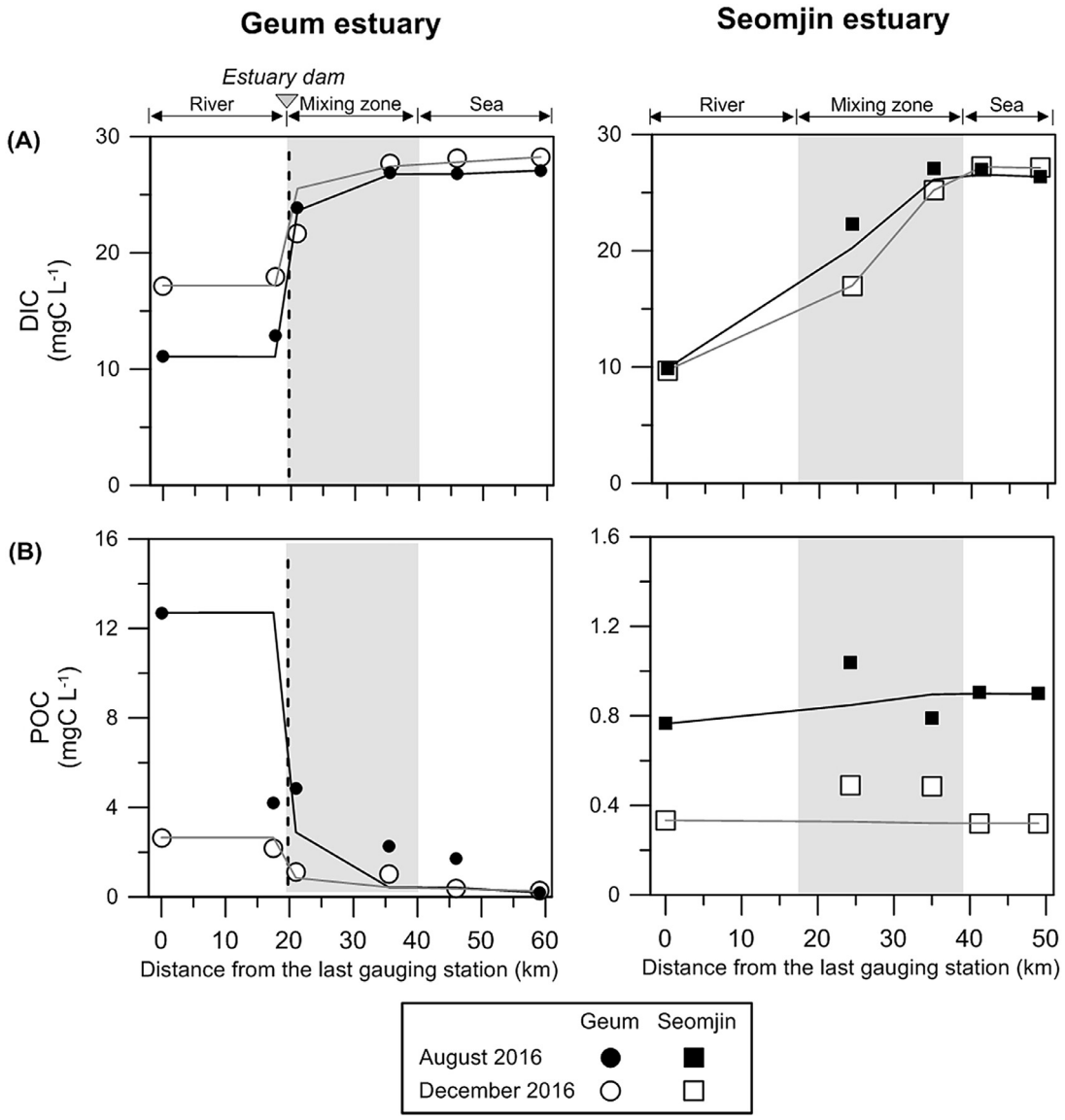

Fig. 5. Variation in (A) DIC concentration (mgC L^{-1}) and (B) POC concentration (mgC L^{-1}) in the Geum and Seomjin estuaries. The lines represent a conservative mix of freshwater and seawater using the end-member compositions, and the symbols indicate calculated or measured values.

Maberly and Madsen, 2002). In general, the $\delta^{13}C$ value of phytoplankton depends on the aquatic $\delta^{13}C_{DIC}$ and subsequent carbon isotope fractionation (on average −21‰) during the assimilation process (e.g., Chanton and Lewis, 1999; Guo et al., 2015; Mackensen and Schmiedl, 2019). At GR1 and GR2, the calculated $\delta^{13}C$ values of phytoplankton based on the measured $\delta^{13}C_{DIC}$ and carbon isotope fractionation (−21‰) values (cf. Guo et al., 2015) were −30.2‰ and −33.0‰ in August 2016 and −29.3‰ and −29.7‰ in December 2016, respectively. Thus, this was within the range (−23‰ to −32‰) of the typical freshwater phytoplankton observed in the various aquatic systems (e.g., Bade et al., 2006; Chanton and Lewis, 1999; Finlay and Kendall, 2007). However, the measured $\delta^{13}C_{POC}$ at GR1 and GR2 in August 2016 (−22.9‰ and −19.4‰, respectively, see Fig. 6) was much higher than the calculated $\delta^{13}C$ of phytoplankton, whereas the measured $\delta^{13}C_{POC}$ values in December 2016 (−28.7‰ and −32.5‰, respectively, see Fig. 6) was similar or slightly depleted compared with the calculated values. Interestingly, the ^{13}C values of phytoplankton can be enriched during the assimilation owing to an increase in water temperature and shift in carbon source from dissolved CO_2 to HCO_3^- when dissolved CO_2 is exhausted due to a heavy phytoplankton bloom, particularly when the Chlorophyta and Cyanophyta are dominant. This is because the $\delta^{13}C$ of HCO_3^- is higher than that of CO_2, and the Chlorophyta and Cyanophyta can directly use HCO_3^- (Wang et al., 2013 and references therein). Although there is no direct information regarding phytoplankton assemblages at our study sites, Chlorophyceae and Cyanophyceae are dominant in the middle reaches of the Geum River in summer (Han et al., 2016). Thus, it seems that the phytoplankton bloom observed at GR1 during the sampling campaign in August 2016 (Kang et al., 2019, 2020) could also be linked to the occurrence of Chlorophyceae and Cyanophyceae, which might have caused a shift from dissolved CO_2 to HCO_3^- in the DIC pool at GR1 and GR2. Accordingly, the higher measured $\delta^{13}C_{POC}$ values as compared with the calculated values at GR1 and GR2 in August 2016 were associated with the enhanced contribution of ^{13}C-enriched phytoplankton-derived POC to the total POC pool. Furthermore, the lower DIC concentrations (on average 12.0 ± 1.2 mgC L^{-1}) at GR1 and GR2 in August 2016 than those (on average, 17.6 ± 0.6 mgC L^{-1}) in December 2016 (see Fig. 5A) were supportive of the phytoplankton bloom in summer,

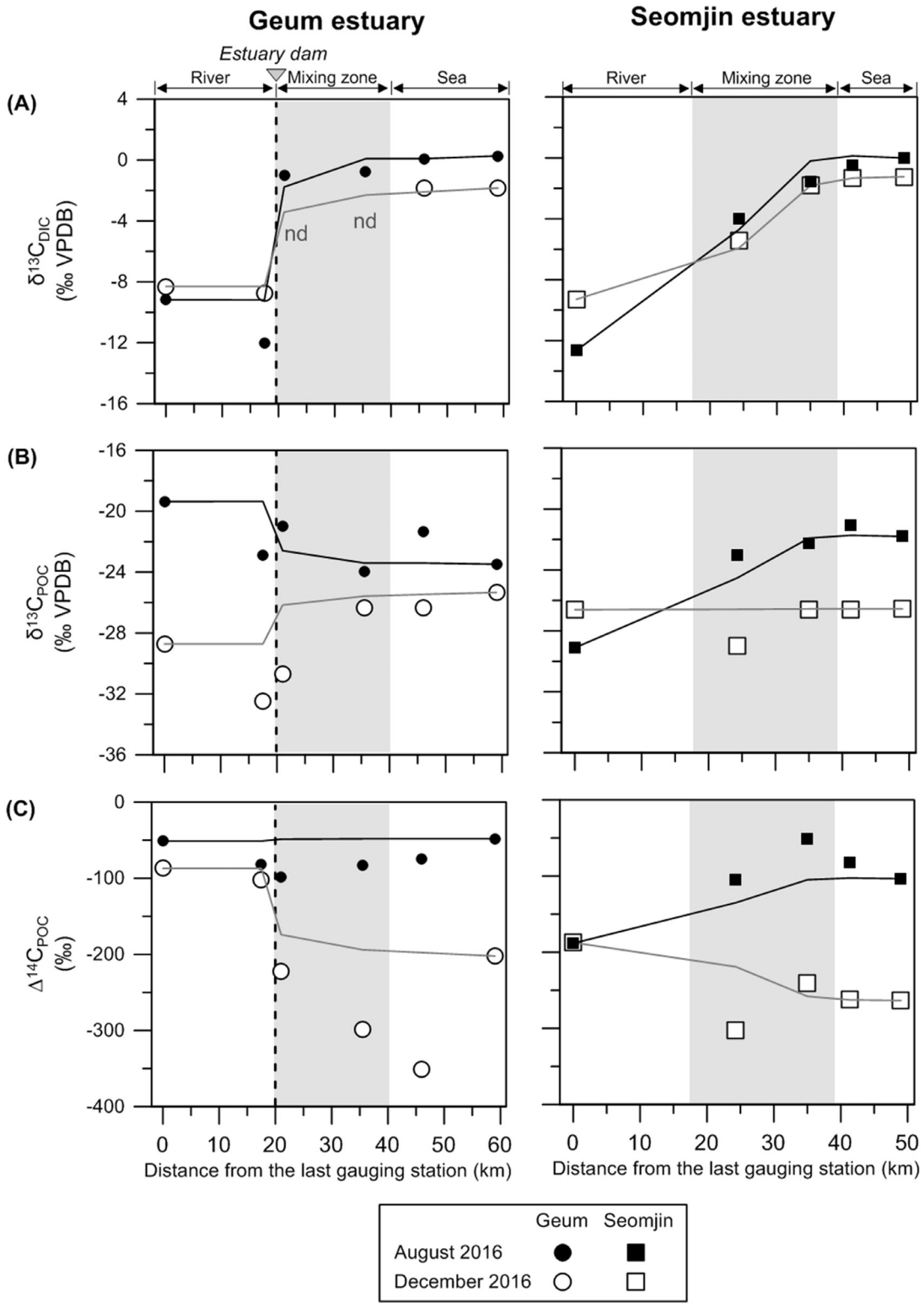

Fig. 6. Variation in (A) $\delta^{13}C_{DIC}$ (‰ VPDB), (B) $\delta^{13}C_{POC}$ (‰ VPDB), and (C) $\Delta^{14}C_{POC}$ (‰) in the Geum and Seomjin estuaries. The lines represent a conservative mix of freshwater and seawater using the end-member compositions, and the symbols indicate the measured values.

as the in situ photosynthesis would result in a decrease in the DIC concentration through the consumption of dissolved CO_2 (e.g., Samanta et al., 2015; Bhavya et al., 2018). In contrast, the seasonal differences in DIC concentration at SJR1 were minor, suggesting the negligible influence of the in situ photosynthesis on DIC concentration for the two sampling periods (see Fig. 5A).

Another piece of evidence supporting the $\delta^{13}C_{POC}$ signatures discussed above can be found in the $\Delta^{14}C_{POC}$ characteristics, which have been commonly used to constrain the source of POC (e.g., Raymond and Bauer, 2001; Wu et al., 2018). Riverine $\Delta^{14}C_{POC}$ values depend on the mean time elapsed because of biosynthesis and the integrated effect of transport or deposition of POC in the

watershed (e.g., Raymond and Bauer, 2001; Hilton et al., 2015; Marwick et al., 2015). Recently fixed terrestrial plants have a high $\Delta^{14}C$ value of 40‰ to 200‰, consistent with the $\Delta^{14}C$ of atmospheric CO_2 (e.g., Marwick et al., 2015; Wu et al., 2018), whereas ancient OC from bedrock weathering and fossil fuels has a $\Delta^{14}C$ value of −1000‰ (e.g., Marwick et al., 2015; Xue et al., 2017; Wu et al., 2018; Yu et al., 2019), and the $\Delta^{14}C$ of soil-derived OC has a wide range between that of ancient OC and that of modern biomass-derived OC (Marwick et al., 2015). Because phytoplankton uses DIC as a carbon source, the $\Delta^{14}C$ of riverine phytoplankton depends on the $\Delta^{14}C$ of DIC in water (Mortazavi and Chanton, 2004; Zigah et al., 2012; Tao et al., 2018). The global mean riverine $\Delta^{14}C_{DIC}$ value was 2‰, although the riverine $\Delta^{14}C_{DIC}$ can be much lower, e.g., −164 to −125‰ in the Yellow River and −137 to −164‰ in the Changjiang River (Marwick et al., 2015; Wang et al., 2016; Tao et al., 2018). The $\Delta^{14}C_{POC}$ values at GR1 and GR2 were higher in August 2016 (−81.7 to −51.1‰) than in December 2016 (−101.8 to −87.0‰, Fig. 6C). Moreover, the $\Delta^{14}C_{POC}$ values were lower at SJR1 (on average −187.8 ± 0.7‰) than at GR1 and GR2 in both seasons (Fig. 6C). To the best of our knowledge, the $\Delta^{14}C$ values of soil OC in the Geum and Seomjin watersheds have not yet been reported; however, the $\Delta^{14}C_{POC}$ value observed in the Seomjin River was slightly higher than the $\Delta^{14}C$ values of soil OC from the Yellow River basin (−510 to −174‰) and the Changjiang River basin (−306 to −246‰) (Xue et al., 2017; Wu et al., 2018; Yu et al., 2019) and, thus, from the Changjiang River (–436 to –103‰; Wang et al., 2012; Wu et al., 2018) and the Yellow River (–635 to –243‰; Wang et al., 2012; Tao et al., 2018). Note that the input of soil-derived OC is higher in the yellow River than in the Changjiang River, resulting in lower $\Delta^{14}C_{POC}$ values (Wang et al., 2012). Accordingly, the $\Delta^{14}C_{POC}$ values at the Geum River sites indicate that the contribution of phytoplankton-derived POC to the total POC pool was higher in August 2016 while a higher input of plant debris decreased the $\Delta^{14}C_{POC}$ values in December 2016. In contrast, for both seasons, the soil-derived OC was the dominant source at the Seomjin River site.

4.2. POC sources within the estuarine region

In general, the POC in the estuary results from the mixing of several OC sources, including riverine (i.e., soils, plants, and freshwater phytoplankton detritus) and in situ phytoplankton (Bianchi and Bauer, 2011 and references therein). After the dam in the Geum estuary system (GR3 to GR6), the POC concentrations were slightly higher in August 2016 than in December 2016 (Fig. 5B). Notably, the TSM concentration at GR3 was much higher in August 2016 than in December 2016, whereas those of other sites were similar for both seasons (Fig. 4F). Considering that the water discharge was higher in August 2016 than in December 2016 (Fig. 2A), it seems that the GR3 site located just after the estuary dam was more strongly influenced by the input of the riverine-derived POC than the other estuary sites. It is also worthwhile to note that the measured POC concentrations were higher than the modeled ones (Fig. 5B). This suggests that in addition to the terrestrial and in situ POC sources, an additional source appears to contribute to the total POC pool in the estuarine region. In the Seomjin estuarine region (SJR2 to SJR5), the POC concentrations were also higher in August 2016 than in December 2016 (Fig. 5B), whereas the TSM concentrations and the water discharges were similar for both seasons (Figs. 2B and 4F). Notably, the measured POC concentrations were, in general, higher than the modeled values in the mixing zone (Fig. 5B). This suggests that besides the riverine and in situ POC sources, an additional POC source contributed to the total POC pool in the Seomjin estuarine region, similar to the case in the Geum estuarine region.

In the Geum estuarine region (GR3 to GR6), $\delta^{13}C_{POC}$ was higher in August 2016 (−22.4 ± 1.5‰) than in December 2016 (−27.2 ± 2.4‰, Fig. 6B). Similarly, in the Seomjin estuarine region (SJR2 to SJR5), $\delta^{13}C_{POC}$ was higher in August 2016 (−22.0 ± 0.8‰) than in December 2016 (−27.2 ± 1.2‰, Fig. 6B). Marine phytoplankton has a $\delta^{13}C_{POC}$ range of −17 to −24‰ (e.g., Chanton and Lewis, 1999; Lamb et al., 2006; Kim et al., 2019; Mackensen and Schmiedl, 2019), which is higher than that of terrestrial-derived POC (e.g., Peterson and Fry, 1987; Meyers, 1997; Marwick et al., 2015). Hence, our results suggest that in both estuarine systems, the contributions of in situ phytoplankton-derived POC were generally higher in August 2016 than in December 2016. It is worthwhile to note that in natural estuaries, an increasing $\delta^{13}C_{POC}$ trend toward the marine sites was observed due to mixing between ^{13}C-depleted terrestrial and ^{13}C-enriched marine POC sources (Wu et al., 2013; Guo et al., 2015). In the Geum estuarine region, such an increasing trend was not observed in August 2016 (Fig. 6B), owing to the high $\delta^{13}C_{POC}$ signature associated with the increased freshwater phytoplankton production before the estuary dam, as discussed in Section 4.1. In contrast, an increasing $\delta^{13}C_{POC}$ trend was observed in December 2016 (Fig. 6B). However, the $\delta^{13}C_{POC}$ of GR3 was much lower than the modeled value but similar to that of GR2 located just before the estuary dam, indicating a strong influence by the GR2 signature at GR3. In the Seomjin estuarine region, $\delta^{13}C_{POC}$ increased toward the marine sites in August 2016 (Fig. 6B). However, such a trend was not observed in December 2016, with similar $\delta^{13}C_{POC}$ values along the estuary gradient, which indicates that the riverine-derived POC was dominant in the total POC pool. Nonetheless, the $\delta^{13}C_{POC}$ value was lower at SJR2 than at other sites, suggesting an additional source besides the riverine- and in situ phytoplankton-derived POC.

Another piece of evidence supporting the enhanced in situ phytoplankton-derived POC contribution in August 2016 over that in December 2016, as discussed above, can be found in the DIC signatures. The $\delta^{13}C_{DIC}$ value in seawater is higher than that of the riverine DIC (−12 to −15‰), ranging from 0 to 2.4‰ (e.g., Chanton and Lewis, 1999; Campeau et al., 2017; Mackensen and Schmiedl, 2019). In natural estuary systems, similar to the case of $\delta^{13}C_{POC}$, an increasing $\delta^{13}C_{DIC}$ trend (−15 to 2.4‰) was observed (e.g., Chanton and Lewis, 1999; Kaldy et al., 2005; Bhavya et al., 2018; He and Xu, 2017). In both estuarine regions, $\delta^{13}C_{DIC}$ was higher in August 2016 than in December 2016, showing an increasing trend toward the marine sites (Fig. 6A). Thus, the calculated $\delta^{13}C$ of phytoplankton (cf. Guo et al., 2015) was slightly higher in August 2016 than in December 2016, with values of −21.4 ± 0.6‰ and −22.8 ± 0‰ in the Geum estuarine region, respectively, and −22.5 ± 1.8‰ and −23.5 ± 2.0‰ in the Seomjin estuarine region, respectively. Thus, the $\delta^{13}C_{DIC}$ signatures are consistent with the measured $\delta^{13}C_{POC}$, suggesting that the contribution of in situ phytoplankton-derived POC was higher in August 2016 than in December 2016 in both estuarine regions.

The $\Delta^{14}C_{POC}$ characteristics in both estuarine regions also exhibited seasonal differences, showing higher values in August 2016 than in December 2016 (Fig. 6C). This is in good agreement with the $\delta^{13}C_{POC}$ signatures discussed above, indicating that the contribution of in situ phytoplankton-derived POC to the total POC pool was higher in August 2016 than in December 2016 in both estuarine regions. Notably, in August 2016, the measured $\Delta^{14}C_{POC}$ values were slightly lower than the modeled values in the Geum estuarine region, whereas they were slightly higher in the Seomjin estuarine region (see also Fig. 6C). This suggests that a contribution of fresher POC to the total POC pool was larger in the mixing zone of the Seomjin estuary, as previously suggested by Kang et al. (2020). In contrast, in December 2016, the measured $\Delta^{14}C_{POC}$ values were generally lower than the modeled values in both estuarine regions.

They were also lower than the global median signature of −230‰ in the estuaries (Marwick et al., 2015). This suggests that besides the riverine- and in situ phytoplankton-derived POC, an additional POC source seems to contribute to the total POC pool.

4.3. Environmental factors influencing POC sources

As can be seen in Figs. 3 and 4, water parameters such as salinity showed an abrupt change from before the dam to after the dam in the Geum estuary system for the two sampling periods, whereas a gradual change was observed in the Seomjin estuary system for both seasons. Hence, it is evident that the Geum estuary dam regulated the salinity diffusion to the upstream region (Cho et al., 2016). Consequently, the upstream of the estuary dam was converted into a lacustrine system (Jeong et al., 2014; Yang, 2014), promoting a phytoplankton bloom in August 2016, as discussed in Section 4.1 (see Figs. 5 and 6). It seems that the phytoplankton bloom caused a pH increase (see Fig. 4C) owing to the fixation of CO_2 by the phytoplankton (Verspagen et al., 2014), which converted the DIC pool into an HCO_3^- dominant one (Wang et al., 2013 and their referencein). A shift in the carbon source from dissolved CO_2 to HCO_3^- could have promoted a Chlorophyceae and Cyanophyceae bloom, increasing the $\delta^{13}C_{POC}$ values in August 2016 (see Fig. 6B). Accordingly, it appears that the Geum estuary dam plays an important role in altering the characteristics of POC transferred to the estuarine region.

The OC degradation increases the DIC concentration and decreases $\delta^{13}C_{DIC}$ because of the selective loss of ^{13}C-enriched labile carbohydrate and amino-acids fractions (e.g., Bellanger et al., 2004). Thus, the deviation of the measured DIC concentration or $\delta^{13}C_{DIC}$ from the modeled values can represent an input or removal of carbon within a system (e.g., Loder and Reichard, 1981; He and Xu, 2017; Oliveira et al., 2017). The differences between the measured and modeled values of the DIC concentration and $\delta^{13}C_{DIC}$ were illustrated as a scatter plot in Fig. 7A. In general, the small deviations from zero of Δ[DIC] and $\Delta[\delta^{13}C_{DIC}]$ suggested that the OC degradation was less important at most of the sites in both the Geum and Somjin estuary systems in August and December 2016. However, the sample at GR2 collected in August 2016 was separately plotted from others in the right lower quadrant, suggesting the occurrence of the OC degradation at this site. The degradable OC at GR2 might be supplied from GR1 where a heavy phytoplankton bloom occurred in August 2016 (Kang et al., 2019; 2020). The Δ[POC] and $\Delta[\delta^{13}C_{POC}]$ values of the sample at GR2 collected in August 2016 were also separately plotted in the lower left quadrant (Fig. 7B), supporting the removal of OC by degradation. Accordingly, it appears that the OC degradation at GR2 was promoted owing to the longer residence time of OC in the Geum reservoir associated with the estuary dam.

Interestingly, the $\Delta[\delta^{13}C_{POC}]$ and $\Delta[\Delta^{14}C_{POC}]$ of the samples collected in both the Geum and Seomjin estuarine regions in December 2016 were mostly negatively plotted (Figs. 7B and C). Furthermore, for both the Geum and Seomjin estuarine regions, the relatively modern POC%, estimated using a simple binary mixing model between the fossil and recently fixed modern (terrestrial, riverine/estuarine, and marine) POC (cf. Kang et al., 2020), was much smaller for the samples collected in December 2016 than those collected in August 2016 (Fig. 8). In contrast, at the Geum and Seomjin river sites, the relatively modern POC% was similar for both sampling periods. As mentioned in Section 4.2, an additional POC source seems to contribute to the total POC pool in the estuarine regions besides the riverine and in situ phytoplankton-derived POC. The resuspension of POC in the estuary occurs related to tidal and wind processes, such as tidal-induced upwelling, wind-induced upwelling, and overturning eddies (e.g., Demers et al., 1987; Bianchi and Bauer, 2011). Indeed, in the Geum and Seomjin estuaries, the resuspension of bottom sediments occurs in association with tidal currents (Jeong et al., 2014; M. Lee et al., 2018). However, a tidal-derived mixing has a relatively short cycle of about 15 days (Cho et al., 2020), and thus would not be responsible for the seasonal contrast in POC characteristics observed in this study. In the study areas, north winds generate large waves, especially during the winter season (Jeong et al., 2014; Wells and Park, 1992; Yang et al., 2003). The average wind speed of previous 14 days at the time of sampling which affected the sediment re-

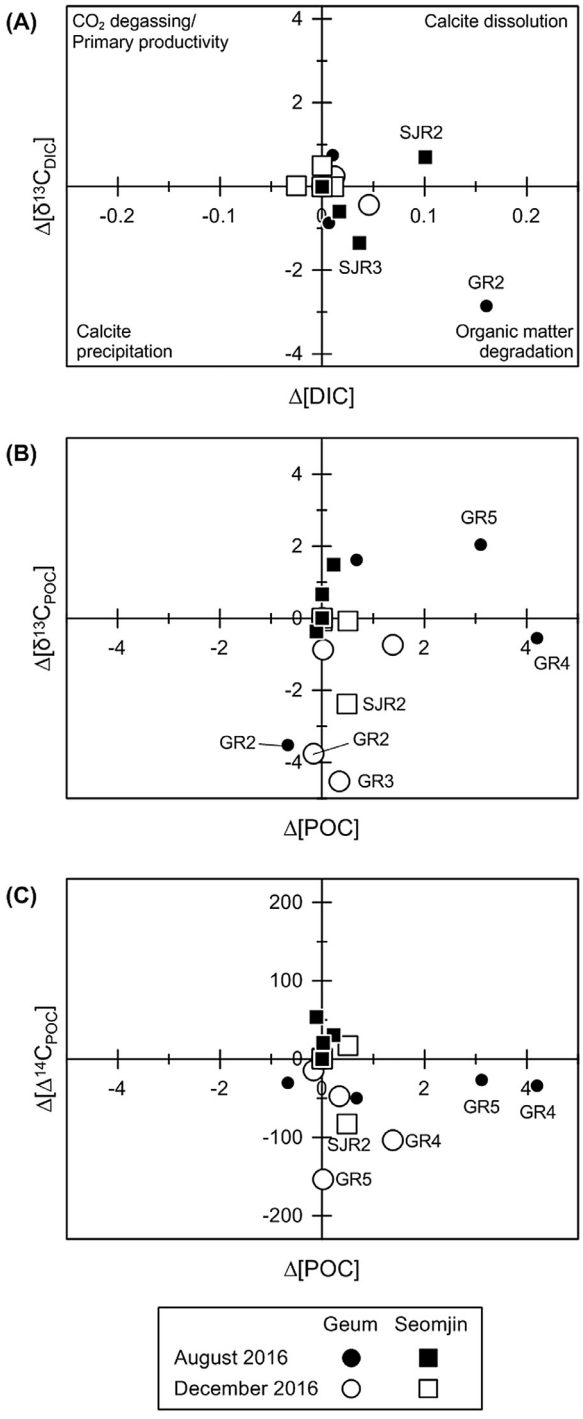

Fig. 7. Deviations in (A) $\delta^{13}C_{DIC}$ (‰ VPDB) versus DIC concentration (mgC L^{-1}), (B) $\delta^{13}C_{POC}$ (‰ VPDB) versus POC concentration (mgC L^{-1}), and (C) $\Delta^{14}C$ (‰) versus POC concentration (mgC L^{-1}) from the corresponding values of the conservative mix in the Geum and Seomjin estuaries.

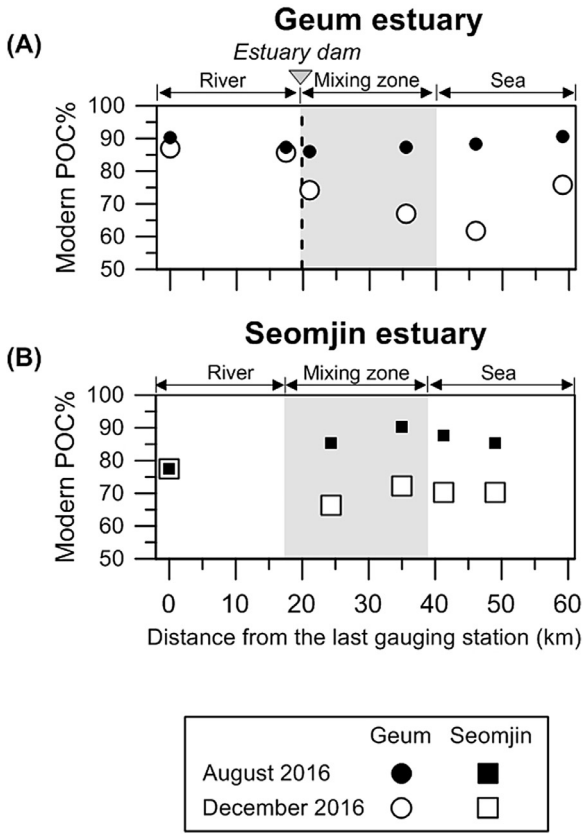

Fig. 8. Relative proportions of modern POC% in the (A) Geum and (B) Seomjin estuaries estimated using a simple binary mixing model (cf. Kang et al., 2020).

suspension (Tammeorg et al., 2013) on the sampling day in December 2016 was higher than that in August 2016 in both Geum and Seomjin estuaries (see Fig. 2B). The stronger wind speed in winter thus resulted in a stronger resuspension of bottom sediments as shown by the enhanced turbidity in December 2016 than in August 2016 (see Figs. 3 and 4). Accordingly, our results suggest that resuspended sediments, which have lower $\Delta^{14}C$ values than those of riverine suspended particulate matter provided a stronger contribution to the total POC pool in both estuarine regions in winter than in summer, owing to the stronger wind-related processes in winter.

5. Conclusion

We investigated surface water samples collected in the two contrasting Korean estuary systems (i.e., closed Geum and open Seomjin estuaries) along a salinity gradient in August and December 2016. The POC concentration, $\delta^{13}C_{POC}$, and $\Delta^{14}C_{POC}$ were higher in August 2016 than in December 2016 at the Geum River sites, which was due to the higher contribution of the phytoplankton-derived POC to the total POC pool in August 2016 associated with the estuary dam. However, at the Seomjin River site, the $\delta^{13}C_{POC}$ value was lower in August 2016 than in December 2016, while the TSM and DIC concentrations, water discharge, and $\Delta^{14}C_{POC}$ were similar for both the seasons except for the POC concentration. This suggests that the contribution of fresher plant-derived POC to the total POC pool was higher in August 2016 than in December 2016 at the Seomjin River site, which was related to the occurrence of local C_3 plant (i.e., *Phragmites australis*). In both estuarine regions, the POC concentration, $\delta^{13}C_{POC}$, and $\Delta^{14}C_{POC}$ were higher in August 2016 than in December 2016. Furthermore, the relatively modern POC% estimated using a simple binary mixing model between fossil and recently fixed modern (terrestrial, riverine/estuarine, and marine) POC was much higher in August 2016 than in December 2016. Given that the relatively modern POC% was similar for both sampling periods, an additional POC source seems to contribute to the total POC pool, along with the riverine and in situ phytoplankton-derived POC, especially in winter. Accordingly, our results suggest that the seasonal characteristics of POC at the river sites were strongly influenced by the presence of the estuary dam. However, wind-induced sediment resuspensions played a more important role in causing the seasonal contrast in POC characteristics in both estuarine regions. Accordingly, our results provide valuable background information on efficient management and preservation of the Geum and Seomjin estuarine ecosystems.

Declaration of Competing Interest

The authors declare that they have no known competing financial interests or personal relationships that could have appeared to influence the work reported in this paper.

Acknowledgements

We are grateful two anonymous reviewers for their constructive comments. We also thank Dong-Hun Lee, Jong-Ku Gal, and Hyuntai Choi for their assistance during fieldwork. This work was supported by the National Research Foundation of Korea (NRF) grants funded by the Ministry of Science and ICT (MSIT) of Korea [NRF-2016R1A2B3015388, KOPRI-PN19100 and NRF-2015M1A5A1037243, KOPRI-PN20090]. This work was also supported by the Korea Environment Industry and Technology Institute (KEITI) through Technology Development Project for Safety Management of Household Chemical Products Progect, funded by the Ministry of Environment (MOE) of Korea [2020002970007, 1485017188].

References

Bade, D.L., Pace, M.L., Cole, J.J., Carpenter, S.R., 2006. Can algal photosynthetic inorganic carbon isotope fractionation be predicted in lakes using existing models? Aquat. Sci. 68, 142–153. https://doi.org/10.1007/s00027-006-0818-5.

Bauer, J.E., Cai, W.-J., Raymond, P.A., Bianchi, T.S., Hopkinson, C.S., Regnier, P.A.G., 2013. The changing carbon cycle of the coastal ocean. Nature 504, 61–70. https://doi.org/10.1038/nature12857.

Bellanger, B., Huon, S., Steinmann, P., Chabaux, F., Velasquez, F., Vallès, V., Arn, K., Clauer, N., Mariotti, A., 2004. Oxic-anoxic conditions in the water column of a tropical freshwater reservoir (Peña-Larga dam, NW Venezuela). Appl. Geochem. 19, 1295–1314. https://doi.org/10.1016/j.apgeochem.2003.11.007.

Beusen, A.H.W., Dekkers, A.L.M., Bouwman, A.F., Ludwig, W., Harrison, J., 2005. Estimation of global river transport of sediments and associated particulate C, N, and P. Glob. Biogeochem. Cycles 19. https://doi.org/10.1029/2005GB002453.

Bhavya, P.S., Kumar, S., Gupta, G.V.M., Sudharma, K.V., Sudheesh, V., 2018. Spatio-temporal variation in $\delta^{13}C_{DIC}$ of a tropical eutrophic estuary (Cochin estuary, India) and adjacent Arabian sea. Cont. Shelf Res. 153, 75–85. https://doi.org/10.1016/j.csr.2017.12.006.

Bianchi, T.S., Duan, S., 2006. Seasonal changes in the abundance and composition of plant pigments in particulate organic carbon in the lower Mississippi and Pearl rivers. Estuar. Coast. 29, 427–442. https://doi.org/10.1007/BF02784991.

Bianchi, T.S., Bauer, J.E., 2011. Particulate organic carbon cycling and transformation. In: Wolanski, E, McLusky, DS (Eds.). In: Treatise on Estuarine and Coastal Science, 5, pp. 69–117.

Bouchez, J., Gaillardet, J., France-Lanord, C., Maurice, L., Dutra-Maia, P., 2011. Grain size control of river suspended sediment geochemistry: clues from Amazon river depth profiles. Geochem. Geophys. Geosy. 12, 1–24. https://doi.org/10.1029/2010GC003380.

Cai, Y., Shim, M.J., Guo, L., Shiller, A., 2016. Floodplain influence on carbon speciation and fluxes from the lower Pearl river, Mississippi. Geochim. Cosmochim. Acta 186, 189–206. https://doi.org/10.1016/j.gca.2016.05.007.

Campeau, A., Wallin, M.B., Giesler, R., Löfgren, S., Mörth, C.M., Schiff, S., Venkiteswaran, J.J., Bishop, K., 2017. Multiple sources and sinks of dissolved inorganic carbon across Swedish streams, refocusing the lens of stable C isotopes. Sci. Rep. 7, 1–14. https://doi.org/10.1038/s41598-017-09049-9.

Chanton, J.P., Lewis, F.G., 1999. Plankton and dissolved inorganic carbon isotopic composition in a river-dominated estuary: Apalachicola Bay, Florida. Estuaries 22, 575–583. https://doi.org/10.2307/1353045.

Cho, E.B., Cho, Y.K., Kim, J., 2020. Enhanced exchange flow during spring tide and its cause in the Sumjin river estuary, Korea. Estuaries Coasts 43, 525–534. https://doi.org/10.1007/s12237-019-00636-9.
Cho, J., Song, Y., Kim, T.I., 2016. Numerical modeling of estuarine circulation in the Geum river estuary, Korea. Procedia Eng. 154, 982–989. https://doi.org/10.1016/j.proeng.2016.07.586.
Choi, W.J., Ro, H.M., Chang, S.X., 2005. Carbon isotope composition of Phragmites australis in a constructed saline wetland. Aquat. Bot. 82, 27–38. https://doi.org/10.1016/j.aquabot.2005.02.005.
Demers, S., Therriault, J.-C, Bourget, E., Bah, A., 1987. Resuspension in the shallow sublittoral zone of a macrotidal estuarine environment: wind influence. Limnol. Oceanogr. 32, 327–339. https://doi.org/10.4319/lo.1987.32.2.0327.
Finlay, J.C., Kendall, C., 2007. Stable isotope tracing of temporal and spatial variability in organic matter sources to freshwater ecosystems. Stable Isotopes in Ecology and Environmental Science, Second Edition Blackwell Publishing, Hongkong.
Guo, W., Ye, F., Xu, S., Jia, G., 2015. Seasonal variation in sources and processing of particulate organic carbon in the Pearl river estuary, South China. Estuar. Coast. Shelf Sci. 167, 540–548. https://doi.org/10.1016/j.ecss.2015.11.004.
Han, S.R., Cho, K., Yoon, J., Lee, J., Yoo, S., Choi, I., Joo, H., Cheon, S., Lim, B.Environment, R., 2016. Phytoplankton community structure of midstream of Geum river on 2014 and 2015. Korean J. Ecol. Environ. 49, 375–384. https://doi.org/10.11614/KSL.2016.49.4.375.
He, S., Xu, Y.J., 2017. Assessing dissolved carbon transport and transformation along an estuarine river with stable isotope analyses. Estuar. Coast. Shelf Sci. 197, 93–106. https://doi.org/10.1016/j.ecss.2017.08.024.
Hedges, J.I., Keil, R.G., Benner, R., 1997. What happens to terrestrial organic matter in the ocean? Org. Geochem. 27, 195–212. https://doi.org/10.1016/S0146-6380(97)00066-1.
Hilton, R.G., Galy, V., Gaillardet, J., Dellinger, M., Bryant, C., O'Regan, M., Gröcke, D.R., Coxall, H., Bouchez, J., Calmels, D., 2015. Erosion of organic carbon in the arctic as a geological carbon dioxide sink. Nature 524, 84–87. https://doi.org/10.1038/nature14653.
Hoffman, J.C., Bronk, D.A., 2006. Interannual variation in stable carbon and nitrogen isotope biogeochemistry of the Mattaponi river, Virginia. Limnol. Oceanogr. 51, 2319–2332. https://doi.org/10.4319/lo.2006.51.5.2319.
Jeong, Y.H., Yang, J.S., Park, K., 2014. Changes in water quality after the construction of an estuary dam in the Geum river estuary dam system, Korea. J. Coast. Res. 30, 1278–1286. https://doi.org/10.2112/jcoastres-d-13-00081.1.
Kaldy, J.E., Cifuentes, L.A., Brock, D., 2005. Using stable isotope analyses to assess carbon dynamics in a shallow subtropical estuary. Estuaries 28, 86–95. https://doi.org/10.1007/BF02732756.
Kang, S., Kim, J.-H., Kim, D., Song, H., Ryu, J.S., Ock, G., Shin, K.H., 2019. Temporal variation in riverine organic carbon concentrations and fluxes in two contrasting estuary systems: Geum and Seomjin, South Korea. Environ. Int. 133, 105126. https://doi.org/10.1016/j.envint.2019.105126.
Kang, S., Kim, J.-H., Ryu, J.S., Shin, K.H., 2020. Dual carbon isotope ($\delta^{13}C$ and $\Delta^{14}C$) characterization of particulate organic carbon in the Geum and Seomjin estuaries, South Korea. Mar. Pollut. Bull. 150, 110719. https://doi.org/10.1016/j.marpolbul.2019.110719.
Kim, C., Kang, H.Y., Lee, Y.J., Yun, S.G., Kang, C.K., 2019. Isotopic variation of macroinvertebrates and their sources of organic matter along an estuarine gradient. Estuar. Coast.. https://doi.org/10.1007/s12237-019-00543-z.
Korea Meteorological Mdministration (KMA) http://www.weather.go.kr, Accessed date: 9 September 2020.
Lamb, A.L., Wilson, G.P., Leng, M.J., 2006. A review of coastal palaeoclimate and relative sea-level reconstructions using $\delta^{13}C$ and C/N ratios in organic material. Earth-Sci. Rev. 75, 29–57. https://doi.org/10.1016/j.earscirev.2005.10.003.
Lee, M., Park, B.S., Baek, S.H., 2018. Tidal influences on biotic and abiotic factors in the Seomjin river estuary and Gwangyang Bay, Korea. Estuaries Coasts 41, 1977–1993. https://doi.org/10.1007/s12237-018-0404-9.
Lee, S.-Y., Jang, R., Han, Y., Jung, Y., Lee, S.-I., Lee, E., You, Y., 2018. Health condition assessment using the riparian vegetation index and vegetation analysis of Geumgang mainstream and Mihocheon. Korean J. Environ. Ecol. 32, 105–117. https://doi.org/10.13047/KJEE.2018.32.1.105.
Lee, Y.G., Kang, J.H., Ki, S.J., Cha, S.M., Cho, K.H., Lee, Y.S., Park, Y., Lee, S.W., Kim, J.H., 2010. Factors dominating stratification cycle and seasonal water quality variation in a Korean estuarine reservoir. J. Environ. Monit. 12, 1072–1081. https://doi.org/10.1039/b920235h.
Loder, T.C., Reichard, R.P., 1981. The dynamics of conservative mixing in estuaries. Estuaries 4, 64–69. https://doi.org/10.2307/1351543.
Ludwig, W., Probst, J.L., 1996. Predicting the oceanic input of organic carbon by continental erosion. Glob. Biogeochem. Cycles 10, 23–41. https://doi.org/10.1029/95GB02925.
Maberly, S.C., Madsen, T.V., 2002. Functional plant biology freshwater angiosperm carbon concentrating mechanisms: processes and patterns. Funct. Plant Biol. 29, 393–405. https://doi.org/10.1071/PP01187.
Mackensen, A., Schmiedl, G., 2019. Stable carbon isotopes in paleoceanography: atmosphere, oceans, and sediments. Earth-Sci. Rev. 197, 102893. https://doi.org/10.1016/j.earscirev.2019.102893.
Marwick, T.R., Tamooh, F., Teodoru, C.R., Borges, A.V., Darchambeau, F., Boillon, S., 2015. The age of river-transported carcon: a global perspective. Glob. Biogeochem. Cycles 29, 122–137. https://doi.org/10.1002/2014GB004911.Received.
Meybeck, M., 1982. Carbon, nitrogen, and phosphorus transport by world rivers. Am. J. Sci. 282, 401–450. https://doi.org/10.2475/ajs.282.4.401.
Meyers, P.A., 1997. Organic geochemical proxies of paleoceanographic, paleolimnologic, and paleoclimatic processes. Org. Geochem. 27, 213–250. https://doi.org/10.1016/S0146-6380(97)00049-1.
Min, B.M., Je, J.-G., 2002. Typical coastal vegetation of Korea. Ocean Polar Res 24, 79–86. https://doi.org/10.4217/OPR.2002.24.1.079.
Mortazavi, B., Chanton, J.P., 2004. Use of Keeling plots to determine sources of dissolved organic carbon in nearshore and open ocean systems. Limnol. Oceanogr. 49, 102–108. https://doi.org/10.4319/lo.2004.49.1.0102.
Oliveira, A.P., Cabeçadas, G., Mateus, M.D., 2017. Inorganic carbon distribution and CO_2 fluxes in a large European estuary (Tagus, Portugal). Sci. Rep. 7, 1–14. https://doi.org/10.1038/s41598-017-06758-z.
Peterson, B.J., Fry, B., 1987. Stable isotopes in ecosystem studies. Annu. Rev. Ecol. Syst. 18, 293–320. https://doi.org/10.1146/annurev.es.18.110187.001453.
Raymond, P.A., Bauer, J.E., 2001. Use of ^{14}C and ^{13}C natural abundances for evaluating riverine, estuarine, and coastal DOC and POC sources and cycling: a review and synthesis. Org. Geochem. 32, 469–485. https://doi.org/10.1016/S0146-6380(00)00190-X.
Samanta, S., Dalai, T.K., Pattanaik, J.K., Rai, S.K., Mazumdar, A., 2015. Dissolved inorganic carbon (DIC) and its $\delta^{13}C$ in the Ganga (Hooghly) river estuary, India: evidence of DIC generation via organic carbon degradation and carbonate dissolution. Geochim. Cosmochim. Acta 165, 226–248. https://doi.org/10.1016/j.gca.2015.05.040.
Sand-Jensen, K., Pederson, M.F., Nielsen, S.L., 1992. Photosynthetic use of inorganic carbon among primary and secondary water plants in streams. Freshwater Biol. 27, 283–293. https://doi.org/10.1111/j.1365-2427.1992.tb00540.x.
Tammeorg, O., Niemistö, J., Möls, T., Laugaste, R., Panksep, K., Kangur K., 2013. Wind-induced sediment resuspension as a potential factor sustaining eutrophication in large and shallow lake Peipsi 559–570. https://doi.org/10.1007/s00027-013-0300-0
Tao, S., Eglinton, T.I., Zhang, L., Yi, Z., Montluçon, D.B., McIntyre, C., Yu, M., Zhao, M., 2018. Temporal variability in composition and fluxes of Yellow river particulate organic matter. Limnol. Oceanogr. 63, S119–S141. https://doi.org/10.1002/lno.10727.
Verspagen, J.M.H., Van De Waal, D.B., Finke, J.F., Visser, P.M., Van Donk, E., Huisman, J., 2014. Rising CO_2 levels will intensify phytoplankton blooms in eutrophic and hypertrophic lakes. PLoS One 9, e104325. https://doi.org/10.1371/journal.pone.0104325.
Wang, X., Ma, H., Li, R., Song, Z., Wu, J., 2012. Seasonal fluxes and source variation of organic carbon transported by two major Chinese rivers: the Yellow river and Changjiang (Yangtze) river. Glob. Biogeochem. Cycles 26, 1–10. https://doi.org/10.1029/2011GB004130.
Wang, B., Liu, C.Q., Peng, X., Wang, F., 2013. Mechanisms controlling the carbon stable isotope composition of phytoplankton in karst reservoirs. J. Limnol. 72, 127–139. https://doi.org/10.4081/jlimnol.2013.e11.
Wang, X., Luo, C., Ge, T., Xu, C., Xue, Y., 2016. Controls on the sources and cycling of dissolved inorganic carbon in the Changjiang and Huanghe river estuaries, China: ^{14}C and ^{13}C studies. Limnol. Oceanogr. 61, 1358–1374. https://doi.org/10.1002/lno.10301.
Water Environment Information System (WEIS) http://water.nier.go.kr, Accessed date: 3 March 2019.
Water Resources Management Information System (WAMIS) http://www.wamis.go.kr, Accessed date: 3 March 2019.
Wells, J.T., Park, Y.A., 1992. Observations on shelf and subtidal channel flow: implications of sediment dispersal seaward of the Keum river estuary, Korea. Estuar. Coast. Shelf Sci. 34, 365–379. https://doi.org/10.1016/S0272-7714(05)80076-9.
Wood, P.A., 1977. Controls of variation in suspended sediment concentration in the river Rother, West Sussex, England. Sedimentology 24, 437–445. https://doi.org/10.1111/j.1365-3091.1977.tb00131.x.
Wu, Y., Eglinton, T., Yang, L., Deng, B., Montluçon, D., Zhang, J., 2013. Spatial variability in the abundance, composition, and age of organic matter in surficial sediments of the East China Sea. J. Geophys. Res. Biogeosciences 118, 1495–1507. https://doi.org/10.1002/2013JG002286.
Wu, Y., Eglinton, T.I., Zhang, J., Montlucon, D.B., 2018. Spatiotemporal variation of the quality, origin, and age of particulate organic matter transported by the Yangtze river (Changjiang). J. Geophys. Res. Biogeosci. 123, 2908–2921. https://doi.org/10.1029/2017JG004285.
Xue, Y., Zou, L., Ge, T., Wang, X., 2017. Mobilization and export of millennial-aged organic carbon by the Yellow river. Limnol. Oceanogr. 62, S95–S111. https://doi.org/10.1002/lno.10579.
Yang, J.S., 2014. Changed aquatic environment due to an estuary dam : similarities and differences between upstream and downstream. J. Korean Soc. Mar. Environ. Energy 17, 52–62. https://doi.org/10.7846/JKOSMEE.2014.17.1.52.
Yang, S.Y., Jung, H.S., Lim, D., Li, C.X., 2003. A review on the provenance discrimination of sediments in the Yellow sea. Earth-Sci. Rev. 63, 93–120. https://doi.org/10.1016/S0012-8252(03)00033-3.
Yu, M., Eglinton, T.I., Haghipour, N., Montluçon, D.B., Wacker, L., Hou, P., Zhang, H., Zhao, M., 2019. Impacts of natural and human-induced hydrological variability on particulate organic carbon dynamics in the Yellow river. Environ. Sci. Technol. 53, 1119–1129. https://doi.org/10.1021/acs.est.8b04705.
Zigah, P.K., Minor, E.C., Werne, J.P., Leigh McCallister, S., 2012. An isotopic ($\Delta^{14}C$, $\delta^{13}C$, and $\delta^{15}N$) investigation of the composition of particulate organic matter and zooplankton food sources in lake superior and across a size-gradient of aquatic systems. Biogeosciences 9, 3663–3678. https://doi.org/10.5194/bg-9-3663-2012.